Publications of the Korean Astronomical Society
27: 243 ∼ 248, 2012 September

ISSN 1225-1534 (Print)
http://dx.doi.org/10.5303/PKAS.2012.27.4.243

OBSERVATIONS OF STAR FORMATION INDUCED BY GALAXY-GALAXY AND GALAXY-INTERGALACTIC MEDIUM INTERACTIONS WITH AKARI

T. Suzuki[1], H. Kaneda[2], and T. Onaka[3]
[1]Institute of Space and Astronautical Science, Japan Aerospace Exploration Agency, Sagamihara-shi, Kanagawa 252–5210, Japan
[2]Graduate School of Science, Nagoya University, Chikusa-ku, Nagoya 464–8602, Japan
[3] Department of Astronomy, Graduate School of Science, The University of Tokyo, 7-3-1 Bunkyo-ku, Tokyo 113-0033, Japan *E-mail: suzuki@ir.isas.jaxa.jp*
(Received June 30, 2012; Accepted august 22, 2012)

ABSTRACT

Nearby spiral galaxies M101 and M81 are considered to have undergone a galaxy-galaxy interaction. M101 has experienced HI gas infall due to the interaction. With AKARI far-infrared (IR) photometric observations, we found regions with enhanced star forming activity, which are spatially close to regions affected by the interaction. In addition, the relation between the star formation rate (SFR) and the gas content for such regions shows a significant difference from typical spiral arm regions. We discuss possible explanations for star formation processes on a kiloparsec scale and the association with interaction-triggered star formation. We also observed the compact group of galaxies Stephan's Quintet (SQ) with the AKARI Far-infrared Surveyor (FIS). The SQ shows diffuse intergalactic medium (IGM) due to multiple collisions between the member galaxies and the IGM. The intruder galaxy NGC 7318b is currently colliding with the IGM and causes a large-scale shock. The 160 micron image clearly shows the structure along the shock ridge as seen in warm molecular hydrogen line emission and X-ray emission. The far-IR emission from the shocked region comes from the luminous [CII]158 μm line and cold dust ($\sim$ 20 K) that coexist with molecular hydrogen gas. Survival of dust grains is indispensable to form molecular hydrogen gas within the collision age ($\sim$ 5 Myr). At the stage of the dusty IGM environment, [CII] and H_2 lines rather than X-ray emission are powerful cooling channels to release the collision energy.

Key words: infrared: galaxies; galaxies: individual (M101, M81, HCG92); galaxies: interactions; stars: formation

1. INTRODUCTION

The evolution of galaxies is influenced by dynamical interactions with other galaxies and with the surrounding intergalactic medium (IGM). Galaxy collisions can induce not only the luminosity and chemical evolution of galaxies but also the chemical enrichment of the IGM. The inflow of the IGM into a galaxy also impacts on their evolution. Among various processes, in particular, star formation induced by these events is a key component. However, the underlying star formation mechanism is not yet clear. Also, it is an open question how the kinetic energy of collisions is released to form molecular gas and provide a reservoir of fuel for star formation.

Mid- to far-infrared (IR) observations can provide useful information for these studies. In these wavebands, there are gas cooling lines such as H_2 rotational lines, the [OI]63 μm line, and the [CII]158 μm line. Dust emission from spiral galaxies shows warm ($\sim$ 60 K) and cold ($\sim$ 20 K) dust components in general, which can be related to the star formation rate (SFR) of massive stars and gas content, respectively (de Jong

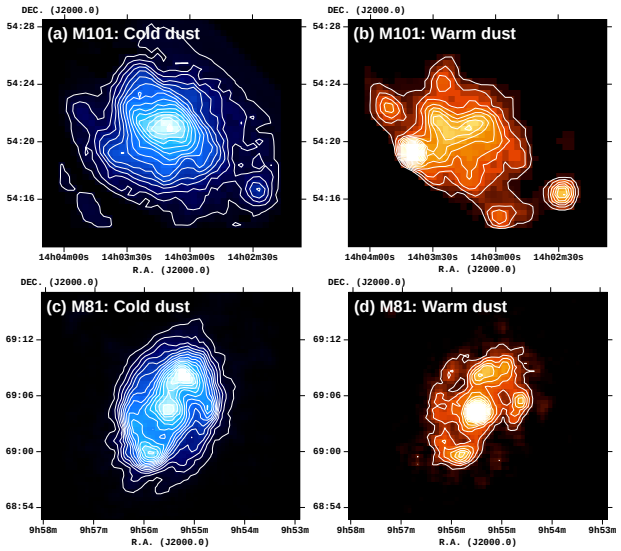

Fig. 1. Spatial distributions of the cold (blue) and warm (red) dust components for M101 (upper panels) and M81 (bottom panels). The contours are linearly spaced from 7% to 98% of the peak with a step of 7%. The peak luminosities for M101 and M81 are 3.1×10^8 $L_\odot$ kpc^{-2} (cold dust), 3.6×10^8 $L_\odot$ kpc^{-2} (warm dust) and 8.5×10^7 $L_\odot$ kpc^{-2} (cold dust), 1.0×10^8 $L_\odot$ kpc^{-2} (warm dust), respectively.

et al., 1984; Cox & Mazger, 1989). The fine allocation of the AKARI/Far-Infrared Surveyor (FIS) four bands can provide spectral information that allows the decomposition of the two dust components. In this paper, we report the observations of interacting/post-interacting galaxies with AKARI/FIS.

2. STAR FORMATION INDUCED BY GALAXY-GALAXY INTERACTIONS

2.1. Post-Interacting Spiral Galaxies: M101 and M81

M101 and M81 are face-on spiral galaxies with global spiral patterns. In M101, there are four giant HII regions (NGC 5447, 5455, 5461, and 5462) on the outskirts of the galaxy, whose star-formation activities are the highest in the galaxy (Suzuki et al., 2007). What triggers the four active giant HII regions is a subject of controversy. As one possibility, it is suggested that intergalactic HI gas might have fallen into the outer disk near NGC 5461 and 5462 (Van der Hulst & Sancisi, 1988) as a result of a past encounter of M101 with its companion dwarf galaxy NGC 5477.

M81 has also experienced tidal interaction with M82. The two galaxies are connected by a stream of HI gas.

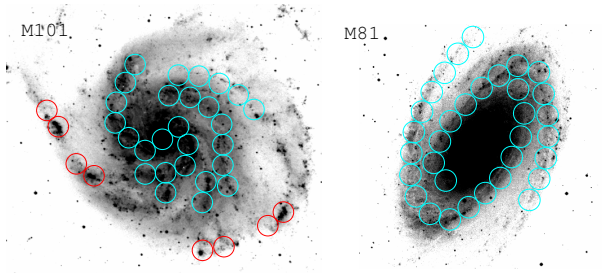

Fig. 2. Field positions in the disks of M101 (left) and M81 (right). The positions of four giant HII regions and contiguous regions are indicated with red circles. Blue circles indicate regions within the spiral arms. The circle's radii are set to 1.0 kpc and 1.2 kpc for M81 and M101, respectively.

Cottrell (1977) investigated the HI velocity field in the region surrounding M81 and M82, concluding that the gas in M82 might be the HI gas captured from the outer parts of M81 during the encounter; the stream of HI gas is in the direction from M81 toward M82. No evidence of the infall of HI gas onto M81 is suggested.

M101 and M81 were observed with AKARI/FIS as part of the FIS calibration program on 2006 June 14 and 2007 April 19, respectively. The FIS was operated in a photometry mode with the four bands: N60 (65 μm), WIDE-S (90 μm), WIDE-L (140 μm), and N160 (160 μm). Details of the observations and data reductions are described in Suzuki et al. (2007, 2010).

2.2. RESULTS

2.2.1. Spatial Distributions of Cold and Warm Dust Components

By using the four-band images, Suzuki et al. (2007, 2010) spectrally decomposed cold and warm dust components of M101 and M81 as shown in Fig. 1. To obtain the spatial distributions of cold and warm dust components, the spatial resolutions of the original WIDE-S and N60 images are reduced to match those of the WIDE-L and N160 images by convolving the former images with a Gaussian kernel. Individual spectral energy distributions (SEDs), constructed from the four-band fluxes at each image bin are fitted with a two-temperature graybody model with an emissivity index of unity, in which only the amplitudes of the blackbodies are set to be free. The temperatures of cold and warm dust components are fixed at the values obtained from the SEDs of the whole galaxies. Four-band flux densities for the whole galaxies are in good agreement

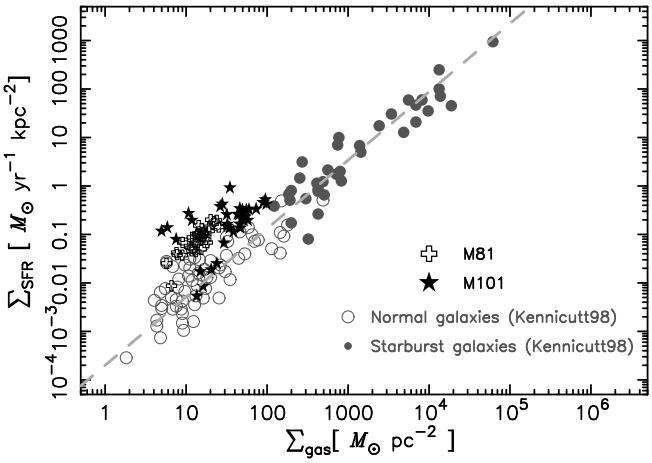

Fig. 3. Relation between gas surface density $\Sigma_{\rm gas}$ and SFR surface density $\Sigma_{\rm SFR}$ in the disks of M101 (stars) and M81 (open crosses). The open and filled circles are infrared-luminous starburst galaxies and normal spiral galaxies from the sample of Kennicutt (1998), respectively. The dashed line shows the power-law model with the index of 1.4.

with those obtained from Spitzer and Herschel observations (Gordon et al., 2008; Bendo et al., 2010; Suzuki et al., 2007, 2010).

Fig. 1 shows that the cold dust component is smoothly distributed over the galaxies, while the warm dust component indicates a correlation with star formation regions. In particular, for M101, four bright spots seen in the warm dust component spatially correspond to four giant HII regions.

2.2.2. *Relation between SFR and Gas Content*

On the basis of the cold and warm dust luminosities in Fig. 1, SFR and gas content for fields within a galactic disk can be estimated by using the following equations (Suzuki et al., 2010);

$$M_{\rm gas}(r,\theta) = GDR(r) M_{\rm C}(r,\theta) \quad (1)$$

and

$$\mathrm{SFR}(r,\theta) = 5.6 \times 10^{-42} 10^{(\log L_{\rm W}(r,\theta) - 0.60)/1.04}, \quad (2)$$

where $M_{\rm gas}$, GDR, $M_{\rm C}$, and $L_{\rm W}$ are the H_2 gas mass, the azimuthally averaged gas-to-dust mass ratio, the cold dust mass, and the warm dust luminosity in polar coordinates, respectively. The relation between SFR and gas surface densities is investigated at various fields as shown in Fig. 2. For M101, the spiral arm regions indicated by the blue circles are defined as the locations at the spiral arms within 5 arcmin from the galactic center. The positions of the red circles spatially correspond to four giant HII regions.

Fig. 3 shows the relation between SFR and gas surface densities within the disks of M101 (stars) and M81 (open crosses) is overplotted on the relation for individual galaxy samples from Kennicutt (1998). Despite the difference in the spatial scale, the *local* relationship for the fields within the disks follows a similar trend as the *global* relationship for individual galaxies: Kennicutt-Schmidt (K - S) law, $\Sigma_{\rm SFR} \propto \Sigma_{\rm gas}^{N} (N = 1.4)$. However, once we focus on the local relationship by regions, the power-law index N varies from 1 to 2 as clearly shown in Fig. 4; the power-law index of the K-S law is not always constant within a galaxy.

2.3. *Star Formation Process Induced by Interactions*

The clear spatial difference in N for M101 may be attributed to the difference in the star formation process on a kiloparsec scale. Van der Hulst & Sancisi (1988) discovered high-speed ($\leq$ 150 km s^{-1}) HI gas falling into the outskirts of the galaxy. The infall may have resulted from the interaction. Santillan et al. (1991) numerically simulated the interaction of high-velocity clouds (200 km s^{-1}) with a magnetized galactic disk. As the gas falls into the disk, perturbation of the magnetic field lines can trigger the Parker instability that creates large magnetic loops above the galactic plane. Then, dense molecular clouds are formed in the gas concentrated at the foot prints of the loops. Once star formation begins by the Parker instability, SFR becomes proportional to the gas density (SFR$\propto \rho_{\rm gas}$, Elmegreen, 1994). The general feature of the spiral arms in M101 can be explained by the density wave theory (Rogstad, 1971). The orbit crowding in spiral arms enhances the number density of gas clouds and thus increases the cloud-cloud collision rate. Scoville et al. (1986) found that the number density of HII regions varies as $\rho_{\rm gas}^2$ (SFR$\propto \rho_{\rm gas}^2$). Thus, with the assumption that the scale height of the disk is constant, the power-law index of unity derived for giant HII regions may be attributed to star formation induced by the Parker instability triggered by the interaction.

Although star formation activities in normal spiral galaxies can be considered to be the highest near the galactic center, star formation activities are surprisingly high in the outskirts of M101 (Suzuki et al., 2007). Therefore, galaxy-galaxy interactions can dramatically

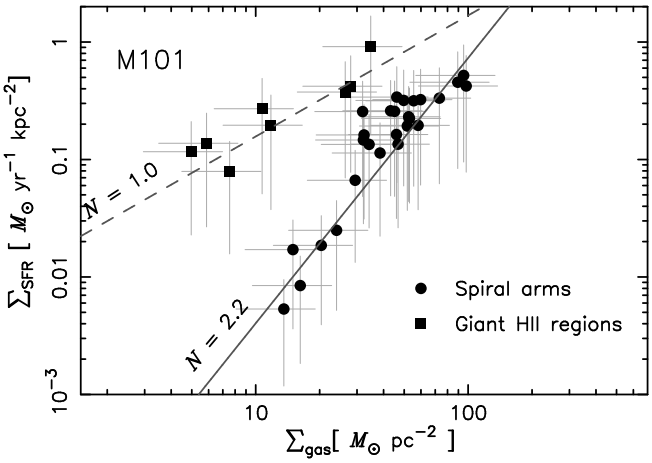

Fig. 4. $\Sigma_{\rm gas}$–$\Sigma_{\rm SFR}$ relations for various regions in M101. Filled circles and boxes show spiral arm regions and the giant HII regions, respectively. The lines and N are the best-fit power-law models and the resulting power-law index, respectively.

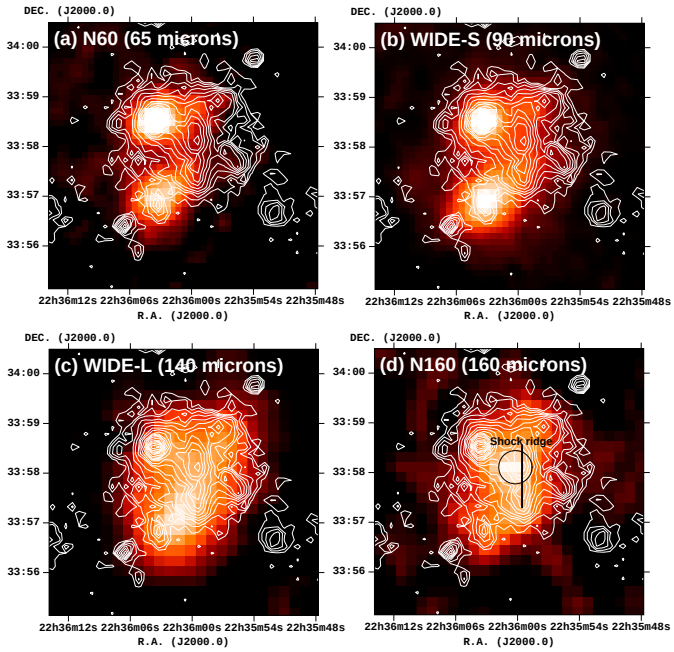

Fig. 5. Four-band images of the SQ overlaid on XMM-Newton X-ray contours. As a reference, the shock ride is shown by the solid black line in the panel (d). The aperture for photometry at the shocked region (r = 20 arcsec) is also shown in the panel (d).

change star formation activities in a galaxy.

3. STAR FORMATION INDUCED BY GALAXY-IGM COLLISION

A compact group of galaxies shows an extreme high density of galaxies that corresponds to the number density at the core region of rich clusters. Compact groups show the chemical enrichment in the IGM by stripping of metal-enriched gas contained in member galaxies. Thus, compact groups in the local universe are unique laboratories to study the effect of the IGM enrichment and to serve as an analogue to the cores of clusters in the early universe.

3.1. Compact Group of Galaxies: Stephan's Quintet

Stephan's Quintet (SQ, HCG92) is a well studied compact group of galaxies with the disturbed IGM. The intruder galaxy NGC 7318b is currently colliding with the IGM at a relative velocity of $\sim$ 1,000 km s^{-1} and causes a large-scale shock front and IGM starbursts (SQ-A and SQ-B). In the shocked region, X-ray emission from shock-heated gas ($\sim 6\times10^6$ K) was detected (e.g. O'Sullivan et al., 2009). Appleton et al. (2006) found powerful H_2 rotational line emission from warm ($\sim$ 10^2–10^3 K) molecular gas in the center of the shock ridge. Cluver et al. (2010) showed that the spatial distributions of H_2 lines were in good agreement with that of X-ray emission. To explain the coexistence of both hot plasma and H_2 gas, Guillard et al. (2009) proposed a model of the shock in the inhomogeneous gas medium; H_2 forms in denser gas clouds experiencing slower shocks ($\sim$ 5–20 km s^{-1}). H_2 line emission is found to have an extremely large line width of 900 km s^{-1}, which reflects the collision velocity, and is extremely luminous. Its luminosity is three times higher than the X-ray luminosity (Cluver et al., 2010). These facts suggest that a large fraction of the collision energy is carried by the kinetic energy of molecular clouds rather than the thermal energy of hot plasma. Although H_2 molecules are likely to be produced on the grain surface (Gould & Salpeter, 1963), direct association of the H_2 gas with dust has yet to be found in the shocked region.

The SQ was observed as part of the AKARI mission program "ISM in our Galaxy and Nearby Galaxies" (ISMGN; Kaneda, 2009) on 2007 Jun 18 using the FIS01 observation mode (Observation ID: 1402238-001). Details of the observations and data reduction are described in Suzuki et al. (2011).

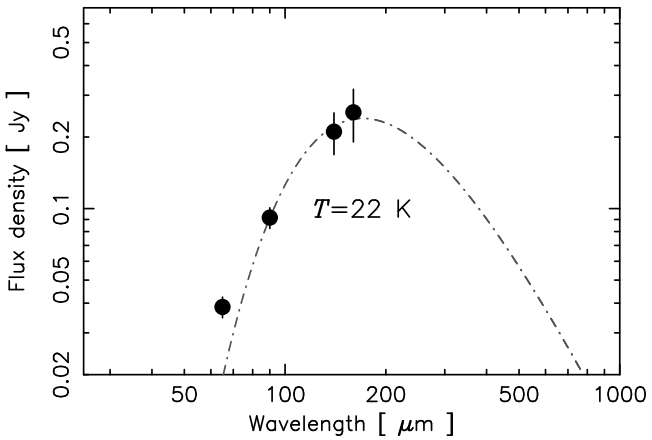

Fig. 6. SED of the shocked region. The position of the aperture is shown in Fig. 5(d). The dash-dotted line shows the best-fit single temperature graybody model.

3.2. Results

3.2.1. Far-IR Four-Band Images

The four-band images are presented in Fig. 5. The N60 and WIDE-S images show prominent emission from NGC 7319, NGC 7320, SQ-A and SQ-B. Although the WIDE-L image shows a structure extending in the North-South direction along the shock ridge, the N160 image clearly shows a single peak emission in addition to the structure, but does not indicate any features associated with the individual galaxies; the spatial distribution of the 160 μm emission is quite similar to that of the X-ray emission in the shocked region. The result clearly shows the spatial correlation of the far-IR emission with the X-ray emission and thus the H_2 line emission.

3.2.2. Far-IR Emission from the IGM

To confirm the origin of the far-IR emission from the shocked region, the SED at the shocked region was investigated by using the four-band images. In Fig. 6, as shown by the dash-dotted line, the SED can be fitted by a single temperature graybody model with the emissivity index of unity and the temperature of $\sim$ 20 K. This means that most of the far-IR emission seen in the N160 band image comes from thermal emission from cold dust grains. From the SED, the far-IR luminosity surface density $\Sigma_{L_{\rm FIR}}$ is estimated to be $(2.0 \pm 0.6) \times 10^{40}$ erg sec^{-1} kpc^{-2} (Suzuki et al., 2010).

Furthermore, we found a dramatic change in the spatial distribution between the 140 μm and 160 μm images. Since the flux ratio between 140 μm and 160 μm is not very sensitive to the dust temperature of $\sim$20 K, the far-IR emission at the shocked region is hard to be explained only by the contribution of cold dust emission. An alternative possibility is a contribution from the shock-powered [CII]158 μm line emission to the 160 μm band. Suzuki et al. (2011) estimated the contribution from the [CII] line. The [CII] luminosity surface density is estimated to be $(1.0^{+0.4}_{-0.5}) \times 10^{39}$ erg sec^{-1} kpc^{-2}, which is comparable to the H_2 line luminosity surface density of 2×10^{39} erg sec^{-1} kpc^{-2} (Cluver et al., 2010) and is $\sim$ 10% of the far-IR luminosity. Suzuki et al. (2011) also estimated the C^+ abundance per hydrogen atom X_{C^+}, with the assumption that the [CII] line emission comes from the warm H_2 gas clouds and is optically thin; X_{C^+} is estimated to be $\sim 1 \times 10^{-4}$ and is in agreement with that in an interstellar gas phase if the carbon in the [CII] line emitting region is all in a singly ionized form. The luminous [CII] line emission from the shocked region is physically plausible provided that C^+ is the main carbon form in the warm H_2 gas clouds.

3.3. Dissipation Pathways of the Collisional Energy

AKARI reveals that the IGM of the SQ is at the stage of the dusty environment. Suzuki et al. (2011) suggest that the far-IR dust emission arises mostly from radiative heating of cold dust in clumpy molecular gas; dust grains with radii smaller than $\sim$ 0.1 μm cannot survive in the hot plasma due to sputtering (Xu et al., 2003). Natale et al. (2010) estimated the contribution of surviving dust luminosity to the far-IR luminosity, which is of the order of 1% ($\sim 10^{38}$ erg sec^{-1} kpc^{-2}). Thus, dust grains are probably not a dominant coolant. At the dusty stage of the IGM, warm H_2 gas ($\sim$ 100 K) can be formed on dust grains as a reservoir of fuel for future star formation once it cools. Current observational results show that [CII] and H_2 lines rather than X-ray emission are dominant cooling channels to release the collisional energy.

4. SUMMARY

In post-interacting spiral galaxies M101 and M81, there are active star forming regions. The local K-S law provides an insight into the association of star formation activities with interactions. Within the disk of M101, the local K-S law clearly shows a different N between four giant HII regions and the spiral arms. The power-law index for the four giant HII regions indicates that

star formation may be triggered by high-velocity gas infall due to the interaction. Their star forming activities are high in spite of being located on the outskirts of the disk. Galaxy-galaxy interactions can dramatically change the star forming activity in a galaxy.

The SQ shows ongoing galaxy-IGM interaction that triggers IGM star formation and large scale shock. At the shocked region, AKARI clearly shows the presence of dust grains that coexist with H_2 gas. This means that the SQ is at the stage of the dusty IGM environment. The single peak emission seen in the 160 μm image indicates the possibility of the luminous [CII] line emission. In the dusty IGM, H_2 can be formed on dust grains as fuel for future star formation. At this stage, [CII] and H_2 lines rather than X-ray emission are powerful cooling channels to release the collision energy.

ACKNOWLEDGEMENTS

The present work is based on observations with AKARI, a JAXA project with the participation of ESA.

REFERENCES

Appleton, P. N., et al., 2006, Powerful High-Velocity Dispersion Molecular Hydrogen Associated with an Intergalactic Shock Wave in Stephan's Quintet, ApJ, 639, L51

Bendo, G. J., et al., 2010, The Herschel Space Observatory View of Dust in M81, A&A, 518, L65

Cluver, M. E., et al., 2010, Powerful H2 Line Cooling in Stephan's Quintet. I. Mapping the Significant Cooling Pathways in Group-wide Shocks, ApJ, 710, 248

Cottrell, G. A., 1977, 21-cm Observations of the Interacting Galaxies M81 and M82, MNRAS, 178, 577

Cox, P. & Mezger, P. G., 1989, The Galactic Infrared/Submillimeter Dust Radiation, A&ARv, 1, 49

de Jong, T., et al., 1984, IRAS Observations of Shapley-Ames Galaxies, ApJ, 278, L67

Elmegreen, B. G., 1994, Starbursts by Gravitational Collapse in the Inner Lindblad Resonance Rings of Galaxies, ApJ, 425, L73

Gordon, K. D., et al., 2008, The Behavior of the Aromatic Features in M101 H II Regions: Evidence for Dust Processing, ApJ, 682, 336

Gould, R. J. & Salpeter, E. E., 1963, The Interstellar Abundance of the Hydrogen Molecule. I. Basic Processes, ApJ, 138, 393

Guillard, P., et al, 2009, H2 Formation and Excitation in the Stephan's Quintet Galaxy-Wide Collision, A&A, 502, 515

Kaneda, H., et al., 2009, AKARI Observations of the ISM in Our Galaxy and Nearby Galaxies, Adv. Space Res., 44, 1038

Kennicutt, Jr., R. C., 1998, The Global Schmidt Law in Star-forming Galaxies, ApJ, 498, 541

Natale, G., et al., 2010, Dust Emission and Star Formation in Stephan's Quintet, ApJ, 725, 955

O'Sullivan, E., et al., 2009, A Chandra X-ray View of Stephan's Quintet: Shocks and Star Formation, ApJ, 701, 1560

Rogstad, D. H., 1971, Aperture Synthesis Study of Neutral Hydrogen in the Galaxy M101: II. Discussion., A&A, 13, 108

Santillán, A., et al., 1999, The Collisions of High-Velocity Clouds with a Magnetized Gaseous Galactic Disk, ApJ, 515, 657

Scoville, N. Z., et al., 1986, High-Mass Star formation due to Cloud-Cloud Collisions, ApJ, 310, L77

Suzuki, T., et al., 2007, Spatial Distributions of Cold and Warm Interstellar Dust in M101 Resolved with AKARI/Far-Infrared Surveyor (FIS), PASJ, 59, 473

Suzuki, T., et al., 2010, Kiloparsec-Scale Star Formation Law in M 81 and M 101 Based on AKARI Far-Infrared Observations, A&A, 521, 48

Suzuki, T., et al., 2011, Far-Infrared Emission from the Intergalactic Medium in Stephan's Quintet Revealed by AKARI, ApJ, 731, L12

Van der Hulst, T. & Sancisi, R., 1988, High-Velocity Gas in M101, AJ, 95, 1354

Xu, C. K., et al., 2003, Physical Conditions and Star Formation Activity in the Intragroup Medium of Stephan's Quintet, ApJ, 595, 665